

# Structural and Finite Element Analysis of Tractor Axle Casing

Rishabh Mishra <sup>1</sup>, Pankaj Sidar <sup>2</sup>, Kamlesh Ratre<sup>3</sup>

<sup>1</sup>M. Tech Scholar, Department of Mechanical Engineering, VEC Ambikapur, C.G. – India

<sup>2</sup>Assistant Professor, Department of Mechanical Engineering, VEC Ambikapur, C.G. – India

<sup>3</sup>Assistant Professor, Department of Mechanical Engineering, VEC Ambikapur, C.G. – India

\*\*\*

**Abstract** - This paper describes the failure analysis of a tractor's axle casing based on a tractor's spline loaded with a trolley. The rationale behind the failure is that the weight transfer from back to front reduces, which is considered a remedial measure for failure.

**Key Words:** Axle Casing, Ansys, Finite Element Analysis, Solid Works,

## 1. INTRODUCTION

A tractor, an off-road vehicle, is any vehicle that can move on paved or gravel surfaces. The engine, gearbox, differential, and axle carrier are directly connected in a tractor to form a single unit. Since the tractor is meant to pull a load, it has been designed to deliver comparatively high torque and low speed.

In addition to the many critical agricultural applications, tractors have various commercial applications, such as haulage operations in sand mining. In the present work, the finite element analysis approach is used to replace the existing axle casing of the tractor. Premature failure that occurs before the expected load cycle is studied during the life of the axle casing.

For example, failure of axle casings is very likely to occur during sand mining operations, where sand is transported by tractor from the river bank for construction purposes. In this case, a tractor is used with a trolley to carry sand. During this operation, the tractor must operate in extreme adverse road conditions and must pull a load of 20 to 27 tonnes - Failure Analysis of Axle Casing of Mahindra Yuvo 575 DI 4WD.

### 1.1 The objective of Research.

- The main objective of this work is to analyze automobile axle casing.
- Modeling axle casing using SOLID WORKS 2017 and ANSYS workbench 2019 R3.
- To study fatigue analysis of the axle casing to find the fatigue life.
- Necessary design changes will be adopted to attain the axle casing's required fatigue life.

### 1.2 Analysis of the Problem

During the forward movement of a front-wheel-drive tractor with a drawbar pull, there is a weight transfer from the front

wheel to the front wheel. As a result, the front wheels develop poor ground contact compared to the front wheels, and the tractor tends to get lifted from the front. When the front wheel gets lifted, the steering does not respond to the operator. Such an incident is risky, and there is a possibility of an accident. The entire load of the tractor and the torsional driving load acts on the axle casing by lifting the front wheel.

The loads acting on the axle casing is-

- Torsional load,
- The self-weight of the tractor.

Due to the repeated application of the above load to the axle casing, the axle casing fails due to fatigue over a period of operation of 600 to 1000 hours.

## 2. MATERIAL PROPERTIES

### Material Properties

Table 1: Material Properties of AISI 1023 carbon steel

Mechanical Properties	Metric
Tensile strength	425 MPa
Yield strength	282.685049 MPa
Shear modulus	80.0 GPa
Bulk modulus	140 GPa
Elastic modulus	204999.998 MPa
Poisson's ratio	0.29
Elongation at break	15%
Reduction of area	40%
Hardness Brinell	121
Hardness, Knoop	140
Hardness, Rockwell B	68
Hardness, Vickers	126
Machinability	65
Density	7858 kg/m <sup>3</sup>
Thermal conductivity	51.9 W/mK

## 3. AXLE CASING MODELING

The axle casing is one of the tractor components that are present in the differential. Its primary function is protecting the differential and axle. This component is mounted on the tractor's back wheels, called Axle casing.

The axle casing is the outer cover of the axle. Its primary function is to protect the axle. The axle casing is attached to the case 5 cases and has an inner circumferential surface, the ring gear is included in the planetary reduction mechanism, the ring gear axle casing is mounted on the inner peripheral surface of the case.

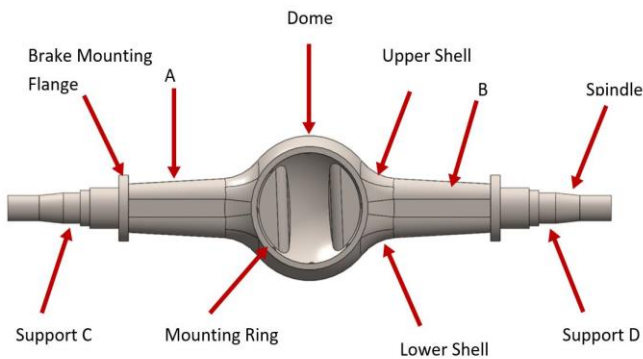


Figure 1. Schematic Diagram of axle casing

3.1 Node and Element Loads:

Loading is defined in two ways: Node and Element. Nodal loads are defined on nodes and are not directly related to elements. These nodals are linked to the DoF at the load node. Elemental weight is surface load, body weight and inertial load. Some elements can even have "flags". Flags are not loaded but indicate that a particular calculation is to be performed.

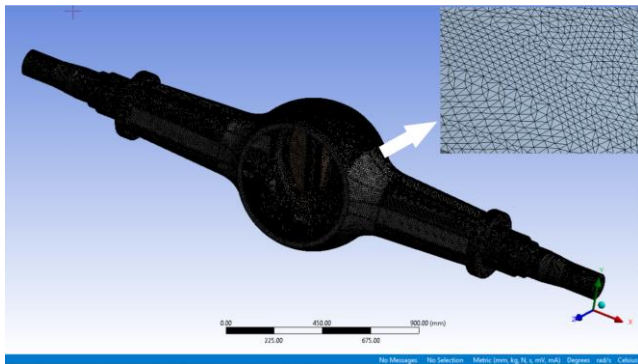


Figure 2. Meshing of axle casing model

Then the node pattern becomes I, J, K, K. If L node is not input, it defaults to node K. If additional size functions are included in the element, they are automatically suppressed (the element is renumbered to a lower order). The specified element load on a nodal basis should have the same load specified at the exact node locations.

4. FINITE ELEMENT MODEL

As shown in Fig 3, a full-scaled CAD model of the casing was prepared for the analyses. The casing essentially consists of two identical thin-walled shells, 9.5 mm thick and welded

along the neutral axis of the spindle. A mounting ring is welded to the casing assembly to increase rigidity on the front side, and the differential carrier is bolted on it. For sealing reasons, a dome is welded to the front side.

Here, elements A and B represent trailing arm-caliper connections. Here, elements A and B represent the trailing arm-caliper connection. Supports C and D stand for wheeled-road contacts. The distance between the support-casing contact points is equal to that of the wheel track of the axle. The solid model of the casing was composed via Solid Works 2017. CAD model of the complete casing was imported into ANSYS Workbench 2019 R3 preprocessing environment to constitute the FE model required in the analyses.

The finite element model casing was meshed using SOLID187, a higher-order three-dimensional solid element with a quadratic displacement behavior and is well suited to irregular model meshes. The element is defined by ten nodes having three translational DOF at each node. The elements CONTA174 and TARGE170 were used to model the contact between the structural parts of the casing. The fully bonded contact was chosen as the contact condition for all welded surfaces. The FE model included 779,305 elements and 1,287,354 nodes.

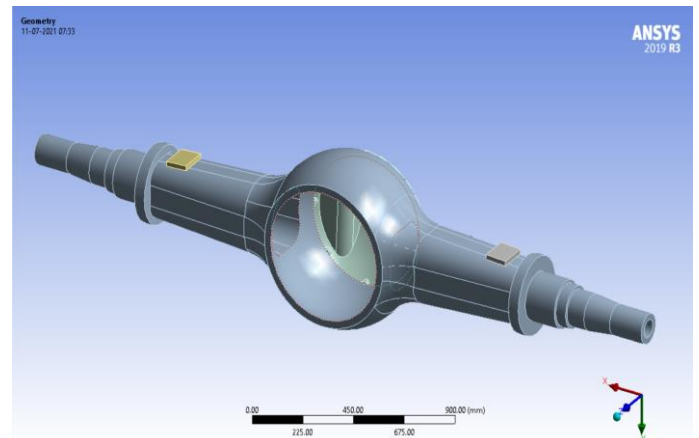
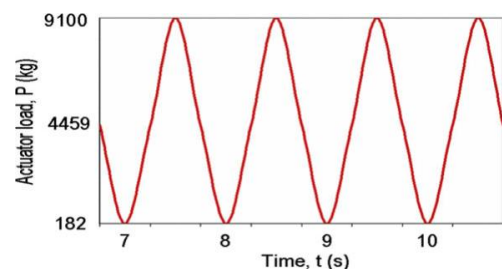


Figure 3. Finite Element Model

5. FINITE ELEMENT ANALYSIS AND RESULTS

FE analysis was used to estimate the precise location of regions where tensile stress concentrations were observed, and the fatigue life is relatively short.



Analysis was carried out using ANSYS Workbench 2019 R3. Fig. 5 shows the equivalent von Mises stress distribution of the FE analysis. Locations of the critical regions and the premature fatigue failure are the same as seen in Fig. 5. The calculated maximum von Mises stress is  $\sigma_{max} = 388.7$  MPa; 78.1% of the yielding point of material. This means that the casing prototype satisfies the safety conditions for maximum loading if it is exerted statically.

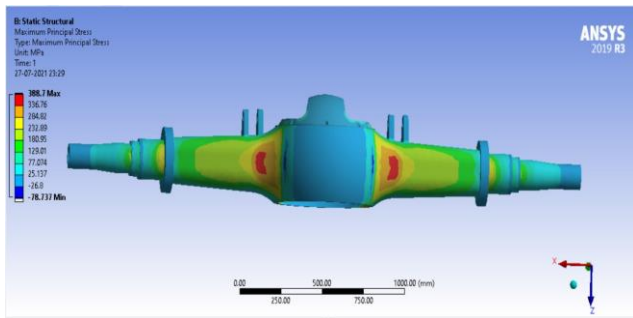


Figure 4. Maximum Principal Stress

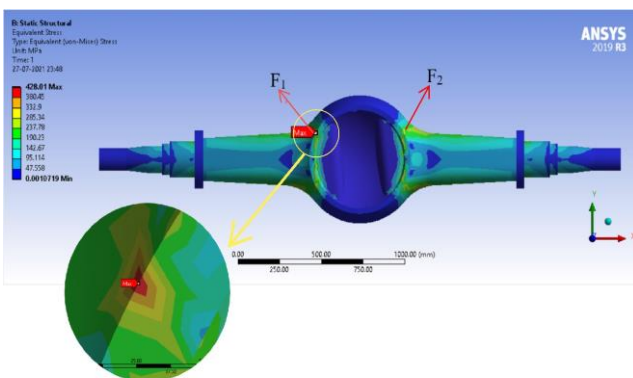


Figure 5. Von-Mises Stress

## 6. FATIGUE LIFE PREDICTION

T fatigue analysis was also performed since the axle casing is loaded with dynamic forces during service. An estimation of the stress life endurance limit  $S_e$  is given as

$$S_e = 0.504 S_{ut}$$

The ultimate strength ( $S_{ut}$ ) of steel is less than 1400 MPa. It represents fatigue strength at  $10^6$  cycles and more. To predict part fatigue life in the range of  $10^5$ – $10^6$  cycles, the casing material's S–N curve was estimated through a practical method that uses data obtained from simple tensile tests.

To predict the true fatigue strength  $S_e$  for a mechanical component,  $S_e$  must be multiplied by several modifying factors representing various design, manufacturing, and environmental influences on the fatigue strength.

$S_e$  is given as

$$S_e = k_b S'_e k_a k_d k_c k_e$$

Since the roughness of the shell surfaces is similar to the hot-rolled sheet after hot stamping, recommended values are

$$a = 57.7 \text{ and } b = 0.718$$

$$k_a = 0.56 \text{ for } S_{ut} = 629.89 \text{ MPa.}$$

In addition, shot peening, a well-known process to introduce favorable residual stresses in the material surface of a component, is also applied on the casing surfaces after hot stamping to increase the fatigue life of the part. In literature, this increase is given by some as 70%. Hence  $k_a = 0.959$  for  $n$  the fatigue analysis.

For non-rounded sections, the shape factor  $k_b$  can be considered as 0.75 for values of the depth of the cross-section  $h$  that exceed 50 mm. Load factor  $k_c$  is given as 1 for bending, and temperature factor  $k_d$  is 1 for the ambient temperature range of  $T = 0 - 250$  °C.

Through static FE analysis, it is observed that the banjo and arm are stress-focused regions at the transition zones. Therefore, in addition to the modifying factors mentioned, a fatigue strength modifying factor  $k_e$  must be considered by means of the static stress concentration factor  $K_t$  that is related to fatigue stress concentration factor  $K_f$ . Hence  $k_e$  is calculated as

$$k_e = 1/K_f$$

For safety reasons,  $K_f$  can be assumed to be equal to  $K_t$ . Because of the dimensions and shape complexity of the casing,  $K_t$  cannot be derived from data in the standard literature.  $K_t$  is defined as

$$K_t = \frac{\sigma_{peak}}{\sigma_{nominal}}$$

where  $\sigma_{peak}$  = peak stress,

$\sigma_{nominal}$  = nominal stress present if a stress concentration did not occur.  $\sigma_{peak}$  was used as the value obtained from static finite element analyses,

$$\sigma_{peak} = \sigma_{max} = 388.7 \text{ MPa.}$$

To calculate  $\sigma_{nominal}$ , the axle was assumed as a simple beam which has a uniform box profile cross-section  $X_1$ – $X_1$  of the critical region along the longitudinal axis  $Y$  and subjected to pure bending.

$$\sigma_{nominal} = M/Z$$

where  $M$  = bending moment and  $Z$  = section modulus of the critical cross-section.

M was obtained as  $41.9 \times 10^6$  N-mm. Section modulus (Z) was calculated,  $Z = 127500 \text{ mm}^3$  and thus  $\sigma_{\text{nominal}} = 329 \text{ MPa}$ .  $K_t \sim K_f = 1.181$  and  $k_e = 0.846$ .

The S-N curve plotted regarding the modifying factors was defined in the ANSYS Workbench 2019 R3 user interface. The stress-life approach was used to determine the fatigue life of the casing material. Von Mises stresses we obtained from finite element analyses are utilized in fatigue life calculations. Since the loading has a sinusoidal fluctuating characteristic (mean stress,  $\sigma_m > 0$ ), modified Goodman approach given as

$$\frac{\sigma_a}{S_e} + \frac{\sigma_m}{S_{ut}} = \frac{1}{n}$$

Here n stands for the factor of safety.

Stress amplitude  $\sigma_a$  is given as

$$\sigma_a = \frac{\sigma_{\text{max}} - \sigma_{\text{min}}}{2}$$

and the mean stress  $\sigma_m$  can be expressed as

$$\sigma_m = \frac{\sigma_{\text{max}} + \sigma_{\text{min}}}{2}$$

Here, both  $\sigma_{\text{max}}$  corresponding to a maximum of 9100 kg and  $\sigma_{\text{min}}$  matching a minimum of 182 kg of vertical load were obtained via FE analysis.

The distribution of n at the lower shell can be seen in Fig. 4. The fatigue analysis results was estimated that crack initiation could occur at the region F<sub>1</sub> of the outer shell surface at  $3.6 \times 10^5$  cycles, which is lower than the expected minimum fatigue life of  $5 \times 10^5$  cycles.

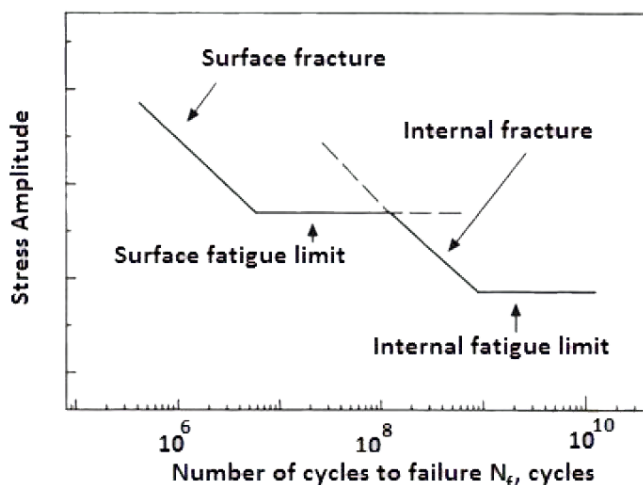


Figure 6. Graph between Stress Amplitude and Number of Cycle to Failure

## 7. RESULTS AND DISCUSSION

FE analysis showed that the regions where fatigue failure was initiated during vertical fatigue tests are subject to stress concentration, leading to premature failure past the estimated  $5 \times 10^5$  minimum cycle limit. The results agree with the results of the vertical fatigue tests.

An increase in the fatigue life of the casing is dependent on a decrease in the stress concentration. However, except in areas F<sub>1</sub> and F<sub>2</sub>, the cover meets the infinite life criterion. An increase in the thickness of the sheet metal leads to an unnecessary increase in weight. For example, a thickness increase of 0.5 mm increases the fatigue limit of the casing material to  $5.8 \times 10^5$  cycles in critical areas that exceed the desired limit. On the other hand, it also means that the weight increases by about 5% of the mass of the vehicle.

As an alternative, the transition geometry can be redesigned. Smooth transition geometry can increase fatigue without adding weight. In addition, the shape of the reinforcement ring also affects the stress concentration. In the studied design, the thickness of the ring is 20 mm. Finite element analysis was repeated for the case without the ring to predict the effects of the ring.

Maximum von Mises stress was obtained as 428.01 MPa at the critical region F<sub>2</sub>. This means the use of the ring decreases stress concentration by about 10%. By increasing the thickness of the part, it is possible to obtain enhanced rigidity. In this design, due to the drivetrain limit configuration, this increased to 5 mm. The static and fatigue analysis was composed according to this change in ring shape. However, analyzes revealed that this increase in itself somewhat prolongs the fatigue life of the casing, which is not sufficient to achieve the desired minimum load cycle of  $5 \times 10^5$ . Therefore, ring thickness enhancement can be implemented with a redesign of the transition geometry.

- a) Maximum von Mises stress was obtained as 428.01 MPa
- b) Desired minimum load cycles of  $5 \times 10^5$
- c)  $\sigma_{\text{nominal}}$  was computed as 329 MPa
- d)  $\sigma_{\text{max}}$  was computed as,  $\sigma_{\text{max}} = 388.7 \text{ MPa}$

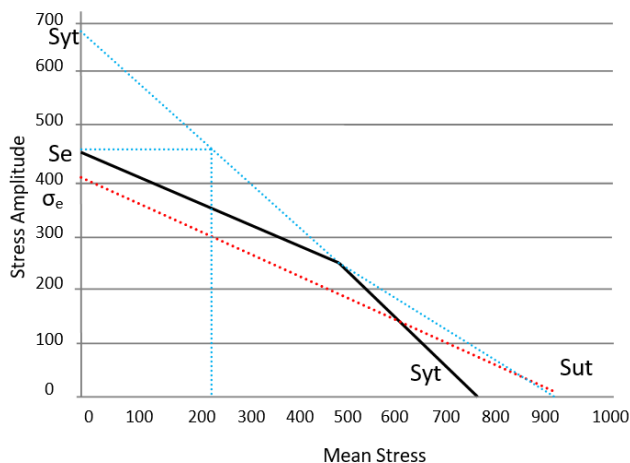


**Figure 7.** Modified goodman plot of mean stress and stress amplitude

Plotting of Stress amplitude and Mean Stress on Modified Goodman Diagram shows that the maximum stress point is inside the safe region. So, Axle casing is safe in both Fatigue and Yield.

Any comparison of materials and their processing to make the final product must be justified by comparing the results of the material and its process under consideration. In the present work, comparative evaluation is done, and results are obtained from the finite element analysis for both existing and modified axle casing.

### 7.1 Concluding Remarks

Premature fatigue failure of an axle casing prototype was examined using finite element analysis. In analyzes in which the vertical fatigue test procedure was simulated, stress-focused areas were predicted in the banjo transition zone. The areas where fatigue cracks occurred were well matched with the analysis results.

Using FE analysis, the location of the failure can be estimated. The determined critical regions are subjected to a combined static and cyclic tensile stress. The crack causing fracture is initiated at the stress-concentrated regions of the casing. Although the casing prototype satisfies the static endurance condition for maximum vertical load, analysis has shown that premature fatigue failure can occur if this load is applied cyclically past the estimated  $5 \times 10^5$  minimum cycle limit.

To solve the problem, increasing sheet metal thickness is not a practical solution because of the weight increase of the casing. An application including redesigning the banjo transition area and increasing the reinforcement ring thickness may be an excellent option to achieve longer fatigue life, which can meet minimum design criteria.

### REFERENCES

- [1]. A. K. P and P. Aswathy, "5 IV April 2017," no. April 2017.
- [2]. A. Kurniawan and Andoko, "Stress and Crack Simulation on Axle Casing Mitsubishi L300 Pickup Car using Finite Element Method," IOP Conf. Ser. Mater. Sci. Eng., vol. 494, no. 1,
- [3]. A. Sciences and I. No, "Optimization of Tractor Trolley Axle for Reducing the Weight and Cost Using Finite Element Method," vol. 2, no. 3, pp. 31-35, 2013.
- [4]. AISI 1023 Carbon Steel (UNS G10230). <https://www.azom.com/article.aspx?ArticleID=6524>
- [5]. Bapi Biswas and Pankaj Sidar, "Parametric stress analysis of helical gear using fea," pp. 1030-1034, 2019. <https://www.irjet.net/archives/V6/i9/IRJET-V6I9153.pdf>
- [6]. F. Hu and W. H. Liu, "Finite element analysis of the tractor front axle casing based on ANSYS," Appl. Mech. Mater., vol. 105-107, pp. 168-171, 2012, doi: 10.4028/www.scientific.net/AMM.105-107.168.
- [7]. Design and Analysis of a Chassis - Term Paper. <https://www.termpaperwarehouse.com/essay-on/Design-And-Analysis-Of-A-Chassis/398364>
- [8]. Design and Analysis of a Chassis - Term Paper. <https://www.termpaperwarehouse.com/essay-on/Design-And-Analysis-Of-A-Chassis/398364>
- [9]. Journal and E. Technologies, "Analysis of Axle Tube and Brake Casing of 65 Hp Tractor," vol. 5, no. 11, pp. 11-17, 2017.
- [10]. Gaur, S. Jain, and A. Khaira, "Design and Analysis of Modified Trumpet Axle," no. 11, pp. 1-3, 2019.
- [11]. O. F. Resource, "MODELLING AND STRUCTURAL ANALYSIS OF REAR Page No : 295," vol. 12, no. 294, pp. 294-302, 2021.
- [12]. R. Alfaro, I. Arana, S. Arazuri, and C. Jarén, "Assessing the safety provided by SAE J2194 Standard and Code 4 Standard code for testing ROPS, using finite element analysis," Biosyst. Eng., vol. 105, no. 2, pp. 189-197, 2010, doi: 10.1016/j.biosystemseng.2009.10.007.
- [13]. Firat, "A computer simulation of four-point bending fatigue of a rear axle assembly," Eng. Fail. Anal., vol. 18, no. 8, pp. 2137-2148, 2011, doi: 10.1016/j.engfailanal.2011.07.005.
- [14]. M. Topaç, H. Günal, and N. S. Kuralay, "Fatigue failure prediction of a rear axle casing prototype by using finite element analysis," Eng. Fail. Anal., vol. 16, no. 5, pp. 1474-1482, 2009, doi: 10.1016/j.engfailanal.2008.09.016.
- [15]. Qinghua, Z. Huifeng, and L. Fengjun, "Fatigue failure fault prediction of truck rear axle casing excited by random road roughness," Int. J. Phys. Sci., vol. 6, no. 7, pp. 1563-1568, 2011, doi: 10.5897/IJPS11.088.

- [16]. M. Meyer, "Effects of Mean Stress and Stress Concentration on Fatigue Behavior of Ductile Iron," no. December 2014.
- [17]. S. Aloni and S. Khedkar, "Comparative Evaluation of Tractor Trolley Axle by Using Finite Element Analysis Approach," *Int. J. Eng. Sci. Technol.*, vol. 4, no. 4, pp. 1351–1360, 2012.
- [18]. S. Shelke and P. Kosbe, "Failure Analysis of Bearing Cup," vol. 3, no. 6, pp. 13634–13641, 2014.
- [19]. Shivaji Nilkanth, Idris Poonawala, and Milind Ramgir, "Design Optimisation of Four Wheel Drive Tractor Front Axle Casing," *Int. J. Eng. Res.*, vol. V4, no. 08, 2015, doi: 10.17577/ijertv4is080114.
- [20]. V. R. Kashid and A. M. Mane, "Finite element analysis and optimization of tractor trolley AXLE," *Int. J. Mech. Eng. Technol.*, vol. 7, no. 4, pp. 48–60, 2016.
- [21]. X. Shao, Z. Song, Y. Yin, B. Xie, and P. Liao, "Statistical distribution modelling and parameter identification of the dynamic stress spectrum of a tractor front driven axle," *Biosyst. Eng.*, vol. 205, pp. 152–163, 2021, doi: 10.1016/j.biosystemseng.2021.03.003.